JBC Papers in Press. Published on February 7, 2014 as Manuscript M113.529735
The latest version is at http://www.jbc.org/cgi/doi/10.1074/jbc.M113.529735

High bone mass in mice lacking Cx37 due to defective osteoclast differentiation*

Rafael Pacheco-Costa[1,2], Iraj Hassan[1], Rejane D. Reginato[2], Hannah M. Davis,[1] Angela Bruzzaniti[3], Matthew R. Allen[1], Lilian I. Plotkin[1]

[1]*Department of Anatomy & Cell Biology, Indiana University School of Medicine, Indianapolis, IN 46202*

[2]*Department of Morphology & Genetics, Federal University of São Paulo School of Medicine, Brazil*

[3]*Department of Oral Biology, Indiana University School of Dentistry, Indianapolis, IN 46202*

* Running title: Cx37 and osteoclast differentiation

To whom correspondence should be addressed: Lilian I. Plotkin. Department of Anatomy and Cell Biology Indiana University School of Medicine 635 Barnhill Drive, MS-5035 Indianapolis, IN, USA, Tel: 317-274-5317; Fax: 317-278-2040; e-mail: lplotkin@iupui.edu

Keywords: gap junctions, connexin37, osteoclast, osteoblast, bone

Background: Connexin proteins are essential for cell differentiation, function and survival.
Results: Global deletion of Cx37 results in increased bone mass due to reduced osteoclast maturation.
Conclusion: Our findings demonstrate a previously unrecognized role of Cx37 in bone homeostasis *in vivo*
Significance: Therapeutic approaches to increase bone mass might be developed by interfering with Cx37 function.

ABSTRACT

Connexin (Cx) proteins are essential for cell differentiation, function and survival in all tissues with Cx43 being the most studied in bone. We now report that Cx37, another member of the connexin family of proteins, is expressed in osteoclasts, osteoblasts and osteocytes. Mice with global deletion of Cx37 ($Cx37^{-/-}$) exhibit higher BMD, cancellous bone volume, and mechanical strength compared to wild type littermates. Osteoclast number and surface are significantly lower in bone of $Cx37^{-/-}$ mice. In contrast, osteoblast number and surface and bone formation rate in bones from $Cx37^{-/-}$ mice are unchanged. Moreover, markers of osteoblast activity *ex vivo* and *in vivo* are similar to those of $Cx37^{+/+}$ littermates. sRANKL/M-CSF treatment of non-adherent $Cx37^{-/-}$ bone marrow cells rendered a 5-fold lower level of osteoclast differentiation compared to $Cx37^{+/+}$ cell cultures. Further, $Cx37^{-/-}$ osteoclasts are smaller and have fewer nuclei per cell. Expression of RANK, TRAP, cathepsin K, calcitonin receptor, MMP9, NFATc1, DCSTAMP, ATP6v0d1 and CD44, markers of osteoclast number, fusion or activity, is lower in $Cx37^{-/-}$ osteoclasts compared to controls. In addition, non-adherent bone marrow cells from $Cx37^{-/-}$ mice exhibit higher levels of markers for osteoclast precursors, suggesting altered osteoclast differentiation. The reduction of osteoclast differentiation is associated with activation of Notch signaling. We conclude that Cx37 is required for osteoclast differentiation and fusion and its absence leads to arrested osteoclast maturation and high bone mass in mice. These findings demonstrate a previously unrecognized role of Cx37 in bone homeostasis that is not compensated for by Cx43 *in vivo*.

Connexins (Cx^{1}) are transmembrane proteins expressed in osteoblasts, osteocytes, and osteoclasts (1). Six connexin proteins arrange in the cell membrane to form hemichannels or connexons. Connexins mediate intercellular communication through gap junction channels formed by two connexons that connect adjacent cells or as unopposed hemichannels, via the release of small molecules to the extracellular

medium (2). The C-terminus of connexin proteins faces the cytoplasm and through interactions with kinases and structural molecules participate in the regulation of intracellular signaling independently of channel activity (3).

Most cells express multiple connexins that form hemichannels composed of one or two different connexins (4). Cx43, for example, can form hemichannels with Cx37, Cx40 or Cx46. In addition, hemichannels composed by one connexin protein in one cell can dock with hemichannels formed by another connexin in a neighboring cell to form heterotypic gap junction channels, which exhibit unique properties, different from channels composed by only one connexin (5).

In bone, Cx43 is the main connexin expressed in osteoblasts, osteocytes and osteoclasts, and it has been the focus of research on the role of this family of proteins in the skeleton (1). A recent gene array study showed that Cx37 (GJA4) is also expressed in bone cells, and it is 5 times more abundant in osteocytes than in osteoblasts (6). However, Cx37 expression in osteoclasts and their precursors has not been examined. In addition, the relative expression level of Cx37 compared to Cx43 in bone, and the role of Cx37 on bone cell function remain unknown.

Cx37 is expressed in monocytes/macrophages, platelets, kidney and ovaries, but it is more abundant in endothelial cells in the blood vessels (7-9). However, Cx37 deletion does not impair vascular function because Cx40, which is also expressed in endothelial cells, can compensate for the absence of Cx37 (10;11). Indeed, double knockout mice lacking both Cx37 and Cx40 die at birth as result of vascular abnormalities. The main phenotypic characteristic of Cx37 null mice is female sterility due to lack of terminal oocyte maturation, absence of ovulation, and accumulation of abnormal corpora lutea. In contrast, male homozygous $Cx37^{-/-}$ and heterozygous $Cx37^{+/-}$ mice breed normally.

Variants of the Cx37 gene are associated with several human diseases. Thus, a Cx37 gene polymorphism resulting from replacement of serine 319 (319S) by proline (319P) in the regulatory cytoplasmic tail is a diagnostic marker for atherosclerosis in humans; with higher risk for myocardial infarction and reduced risk of coronary artery disease in patients carrying the Cx37-319S allele. The increased permeability exhibited by Cx37-319P hemichannels may mediate the differential effects of the two Cx37 polymorphic alleles. In addition, Cx37-319P, but not Cx37-319S, decreases proliferation when transfected into HeLa or SK-HEP-1 cells (12). The proline variant can be phosphorylated by GSK3β, an event that leads to reduced channel activity and decreased proliferation in HeLa cells. Interestingly, the same human gene polymorphism is associated with bone mass in a Japanese population, with men carrying the Cx37-319S allele exhibiting lower total body, lumbar spine, femoral neck, and trochanter BMD (13).

We examined in the current study the skeletal phenotype of mice with global deletion of Cx37. We found that Cx37 is expressed in osteoblasts, osteocytes and osteoclasts, albeit at lower levels than Cx43. Nevertheless, lack of Cx37 impairs osteoclastogenesis, without affecting osteoblast differentiation or function. Our data indicates that reduced bone resorption in Cx37 null mice leads to increased bone mass and bone volume, in particular in cancellous bone of the vertebrae.

EXPERIMENTAL PROCEDURES

Animals–Mice with global deletion of Cx37, generated by A. Simon (14) and provided by J.M. Burt (University of Arizona, Tucson, AZ), were maintained in a C57BL/6 background. Mice expressing green fluorescent protein under the control of the dentin matrix protein 1 promoter (DMP1-GFP) in a C57BL/6 background were previously described (15). All mice were fed a regular diet and water *ad libitum* and maintained on a 12h light/dark cycle. All protocols involving mice were approved by the Institutional Animal Care and Use Committee of Indiana University School of Medicine.

Mice were genotyped by PCR using specific primer sets as follows: wild type allele was detected using 5'-TGC TAG ACC AGG TCC AGG AAC-3' and 5'-GTC CCT TCG TGC CTT TAT CTC-3'; and the mutant allele detected by 5'-GAT CTC TCG TGG GAT CAT TG-3' and 5'-TGC TAG ACC AGG TCC AGG AAC-3'. An amplified fragment of 750bp corresponds to the wild type allele and of 233bp to the mutant allele.

Mice received intraperitoneal injections of calcein (20 mg/kg, Sigma Chemical, St. Louis, MO, USA) and alizarin red (20 mg/kg, Sigma) 7 and 2 days before sacrifice, respectively, to allow for dynamic histomorphometric measurements (16).

Cell preparations and culture–OB-6 osteoblastic cells and MLO-Y4 cells were cultured as previously published (17;18). Immortalized mouse calvaria osteoblastic (MOB) cells were provided by M. M. Thi (Albert Einstein School of Medicine) and cultured in α-MEM containing 10% FBS and 1% penicillin-streptomycin (19). Calvaria cells were isolated from DMP1-8kb-GFP transgenic mice. GFP-expressing cells (osteocyte-enriched) were separated from GFP-negative cells (osteoblast-enriched) by sorting the cell suspension using a FACSAria flow cytometer (BD Biosciences, Sparks, MD) at the Indiana University Flow Cytometry Core Facility, as published (20).

Bone marrow cells were isolated from $Cx37^{+/+}$ and $Cx37^{-/-}$ by flushing the bone marrow out with α-MEM supplemented with 15% FBS and 1% penicillin/streptomycin and then plated at a density of $4x10^5$/cm in 24-well plates for 48h. Non-adherent cells were collected and either plated for osteoclast formation or digested to obtain mRNA. For the osteoclastogenesis assay, $2x10^5$ non-adherent cells/cm^2 were seeded and cultured with 20 ng/ml recombinant murine M-CSF (PeproTech Inc., Rocky Hill, NJ, USA) for 24h. Subsequently, 80 ng/ml recombinant murine sRANKL (PeproTech Inc., Rocky Hill, NJ, USA) was added. Medium was changed every two days for 5 days. Osteoclasts were enumerated after staining for TRAPase using a commercial kit (Sigma-Aldrich Inc., St. Louis, MO, USA.). Images were acquired using a Zeiss Axiovert 35 microscope equipped with a digital camera. mRNA was isolated from parallel cultures and gene expression was measured by quantitative RT-PCR (Applied Biosystems, Foster City, CA).

The number of viable cells was assessed using the MTT assay in cells treated with 30 ng/ml M-CSF for 24h, as previously described (20;21). Cells were pretreated for 1h with vehicle or 2 μM Notch signaling inhibitor GSI XX (Calbiochem, Gibbstown, NJ) (22).

Adherent cells were collected after the initial 48h in culture, plated at a density of $4x10^5/cm^2$ and cultured until reaching 95-100% of confluence. Then, differentiation medium (α-MEM supplemented with 10% FBS, 50μg/ml ascorbic acid and 10mM β-glycerophosphate) was added. Medium was changed every third day. After 14 days in culture cells were stained with Alizarin red for 10 min, as published (23). Images were acquired using a Zeiss Axiovert 35 microscope equipped with a digital camera. After imaging the cells, Alizarin red was dissolved in 10% acetic acid for 30 min at room temperature. The content of the wells were transferred to microtubes and incubated at 85°C for 10 min, followed by centrifugation and neutralization of the supernatants with 10% ammonium hydroxide. Absorbance at 405 nm was measured to estimate the level of mineralization. Parallel cultures were digested to obtain mRNA and perform quantitative RT-PCR (Applied Biosystems, Foster City, CA).

Fluorescent-activated cell sorter (FACS)–Freshly isolated bone marrow cells were incubated with anti–Mac-1-APC (CD11b), and anti-Gr1(granulocyte differentiation antigen 1)-FITC followed by sorting by FACS, as published (24). All antibodies were purchased from e-Biosciences. FACSCalibur and FlowJo were used for acquisition and analysis, respectively.

Whole-mount skeletal staining–Cartilage and mineralized tissue were analyzed in newborn mice using alizarin red/alcian blue staining, as previously published (25). In brief, newborn mice were de-skinned, eviscerated, and kept in 100% ethanol for 48 h. The carcasses were fixed in acetone for 24 h and then stained for 5 days in a solution containing 0.1% alizarin red, 0.3% alcian blue, acetic acid, and 70% ethanol (1:1:1:17, vol/vol/vol/vol). Carcasses were then transferred to a solution of 1% KOH overnight, transferred to a solution of glycerol:KOH (2:8) overnight, and finally to 100% glycerol.

Bone mineral density (BMD) and micro-computed tomography (μCT) analysis–Longitudinal study was performed monthly from 2 to 5 months of age by DEXA using a PIXImus densitometer (G.E. Medical Systems, Lunar Division, Madison, WI) (20). BMD measurements included total BMD

(excluding the head and tail), L1-L6 vertebra (spinal BMD), and entire femur (femoral BMD). For μCT analysis, femora and lumbar vertebrae obtained from male mice at age 2.5 and 5-month were cleaned of adhering tissue and frozen until imaging at 6 μm pixel resolution on a Skyscan 1172 (SkyScan, Kontich, Belgium) (20).

RNA extraction and quantitative RT-PCR (qPCR) –RNA was purified from cells or bones using Trizol reagent (Invitrogen), as previously described (26). qPCR was performed using the house-keeping gene glyceraldehyde 3-phosphate dehydrogenase (GAPDH), and the ΔCt method. Primers and probes were designed using the Assay Design Center (Roche Applied Science, Indianapolis, IN) or were commercially available (Applied Biosystems, Foster City, CA).

Bone histomorphometry–Vertebrae (L6 and L2 for 2.5- and 5-month-old mice, respectively) were dissected, fixed, and embedded in methyl methacrylate. Static historphometric analysis was performed on TRAP stained-sections, as previously described (20). Sequential sections were stained with von Kossa tetrachrome to visualize mineralized bone (16). Dynamic histomorphometric analysis of bone sections was performed on unstained sections, avoiding the primary spongiosa. All measurements were obtained using OsteoMeasure high resolution digital video system (OsteoMetrics Inc., Decatur, GA). The terminology and units used are those recommended by the Histomorphometry Nomenclature Committee of the American Society for Bone and Mineral Research (27).

Biomechanical testing–Femora and lumbar (L5) vertebrae obtained from 5-month-old mice were tested via three-point bending and compression, respectively, following previously published protocols with modifications (28). Briefly, bones were thawed to room temperature, hydrated in 0.9% saline, and loaded to failure at 2 mm/min with force versus displacement data collected at 10 Hz using a servo-hydraulic test system (Test Resources). Femora were loaded to failure in an anterior-posterior direction with the upper contact area at the mid-diaphysis (50% total bone length) and the bottom contact points centered around this point and separated by 8 mm. The posterior processes and end plates were removed prior to testing of the vertebra. Structural mechanical properties, ultimate load, stiffness, and energy to failure were determined from the load-deformation curves using standard definitions while material-level estimations of ultimate stress, modulus, and toughness were calculated using standard equations. Cross-sectional moment of inertia and anterior-posterior diameter were determined by μCT and were used to calculate material-level properties, as previously described (29).

Bone turnover markers–Plasma C-telopeptide fragments (CTX) (RatLaps, Immunodiagnostic Systems Inc., Fountain Hill, AZ, USA), osteocalcin (OCN) (Biomedical Technologies, Soughton, MA, USA) and sclerostin levels (ALPCO Immunoassays, Salem, NH, USA) were measured as described by the manufacturer. Alkaline phosphatase activity was assessed by a standard automated method using a Randox Daytona chemical analyser (Northern Ireland, United Kingdom).

Histological visualization of ovaries–Ovaries were fixed in 3.7% PBS-buffered formaldehyde at room temperature for 48h, followed by transfer to 70% ethanol. Specimens were subsequently dehydrated in ascending ethanol concentrations and embedded in paraffin. 5μm-thick sections were processed for hematoxilin and eosin staining. Images were acquired using an Olympus BX51 TRF microscope equipped with a digital camera.

Statistical analysis–Data were analyzed by using SigmaPlot (Systat Software Inc., San Jose, CA). Differences were evaluated by Student's t-test and considered significant for $p<0.05$. All values are reported as the mean ± standard deviation (SD).

RESULTS

Cx37 is expressed in osteoblasts, osteocytes, and osteoclasts–Gene expression analysis shows that Cx37 is expressed in whole bone at about 4-times lower levels than Cx43 (Fig. 1a). Cx37 can also be detected at much lower levels than Cx43 in the OB-6 osteoblastic cells, in immortalized osteoblastic calvaria cells, and in MLO-Y4 osteocytic cells. In primary osteoblasts, the expression of Cx37 is approximately 300-times

lower than that of Cx43, whereas in primary osteocytes it is approximately 60-times lower (Fig. 1b). In addition, Cx37 is detected in osteoclasts generated by treatment of non-adherent bone marrow cells with M-CSF and sRANKL. In these osteoclast cultures the expression of Cx37 is also lower than Cx43 (approximately 120-fold).

Global deletion of Cx37 in mice leads to high bone mass–Cx37 deficient mice did not exhibit gross abnormalities at birth, and qualitatively appear to have a distribution of cartilage and mineralized bone similar to that of wild type littermates (Fig. 2a). Body weight was similar in male mice from either genotype from 2 to 5 month (Fig. 2b). Femoral length was not different between phenotypes at 5 months of age (15.19 ± 0.27 versus 15.44 ± 0.18 mm for wild type $Cx37^{+/+}$ and $Cx37^{-/-}$ mice, respectively). Female mice exhibit a slight increase in weight at 1 (not shown), 2 and 5 months of age (Fig. 2b).

Male $Cx37^{-/-}$ mice exhibit higher total (5-9%), spinal (11-21%) and femoral (8-21%) BMD compared to wild type littermates at each age examined (Fig. 2c). Female Cx37 deficient mice also exhibit higher bone mass, albeit less than males, with a 3-4% increase in total BMD and a 5-7% increase in femoral BMD at 4 and 5 month of age.

$Cx37^{-/-}$ mice exhibit increased cancellous bone volume and increased mechanical strength in the femur–μCT analysis showed higher bone volume and trabecular number in the cancellous bone of the lumbar vertebra at 2.5 and 5 months of age (Fig. 3a). This was associated with increased trabecular thickness and a tendency towards higher trabecular number in the young animals. In the older mice, only trabecular number was higher. Similar effects of Cx37 deletion were observed in the cancellous bone in the distal femur at 2.5 months of age (Fig. 3b). However, there were no differences between genotypes in 5-month-old mice. Deletion of Cx37 does not result in major changes in cortical architecture or bone material density in the femoral midshaft compared to wild type littermates, with only a slight but significant reduction in cortical thickness (Fig. 3c).

Lumbar vertebrae from Cx37 null mice exhibited higher energy to ultimate load, an indication of the capacity of the bone to resist compression forces (Fig. 4a). Ultimate force and stiffness showed a tendency towards higher values in mice lacking Cx37, but the difference did not reach significance. Deletion of Cx37 resulted in higher cortical bone strength as evidenced by increased ultimate force and mechanical stiffness, compared to wild type littermates in the cortical bone of the femoral midshaft (Fig. 4b). Estimations of material properties, on the other hand, showed no difference between genotypes.

Static histomorphometry revealed lower number of osteoclasts per bone surface (NOc/BS), and reduced bone surface covered by osteoclasts (OcS/BS) and eroded surface (ES/BS) on the vertebral cancellous surface of $Cx37^{-/-}$ mice compared to controls at 2.5 and 5 months of age (Fig. 5a and b). The number of osteoblasts (NOb/BS) and the bone surface covered by osteoblasts (ObS/BS), on the other hand, was not different between genotypes at either age. The lower osteoclast parameters combined with the lack of change on osteoblasts resulted in an increase in quiescent bone surface (QS/BS) in $Cx37^{-/-}$ mice. Dynamic histomorphometry showed no differences in MS/BS, MAR and BFR/BS, parameters which reflect osteoblast number and activity in 5-month-old mice (Fig. 5c).

Differences in circulating markers of bone resorption (CTX) or formation, (osteocalcin and alkaline phosphatase), or in sclerostin, the inhibitor of Wnt signaling, were not detected in either male or female mice at 2, 3 or 5 months of age (Fig. 6).

Deletion of Cx37 decreases osteoclast fusion and differentiation, but does not affect osteoblast differentiation or function–To test the cellular basis for the increased bone mass in the absence of Cx37, we examined osteoclast-specific gene expression in whole bone preparations. As expected, Cx37 expression was undetectable in lumbar vertebrae from $Cx37^{-/-}$ mice, while Cx43 expression was not different from $Cx37^{+/+}$ mice (Fig. 7a). Although the means of the osteoclast-specific genes TRAP and cathepsin K were approximately half in $Cx37^{-/-}$ bones compared to $Cx37^{+/+}$, the difference did not reach significance.

The ability of Cx37-deficient osteoclast precursors to generate mature cells *ex vivo* in the presence of M-CSF and sRANKL was impaired, as evidenced by a lower osteoclast number and size, and number of nuclei/osteoclast (Fig. 7b).

Although, the percentage of CD11b-positive cells (expressing or not the myeloid cell marker Gr1) present in the bone marrow of $Cx37^{-/-}$ mice was similar to $Cx37^{+/+}$ mice, as evidenced by FACS, non-adherent bone marrow cell preparations isolated from $Cx37^{-/-}$ mice exhibited higher expression of osteoclast precursors markers CD11b, CD14 and RANK, compared to cells isolated from wild type littermates (Fig. 7c). These findings suggest that in the absence of Cx37 the expression of osteoclast progenitor-associated genes is increased without a concomitant increase in the abundance of osteoclast precursor cells.

Mature osteoclasts derived from wild type or $Cx37^{-/-}$ mice expressed similar levels of Cx43 mRNA, but expressed reduced levels of osteoclast-specific genes (Fig. 7d). Thus, lack of Cx37 led to a reduction in RANK levels of approximately 30%, whereas the markers of mature osteoclasts TRAP, cathepsin K and calcitonin receptor were all approximately 50% lower. Moreover, NFATc1, a transcription factor essential for osteoclast differentiation induced by RANKL (30), was also lower in Cx37-deficient osteoclasts. Similarly, the expression of dendritic cell-specific transmembrane protein (DC-STAMP) and the d2 isoform of vacuolar ATPase V_o domain (Atp6v0d2), NFATc1 targets that participate in osteoclast fusion, were also reduced. MMP9 and CD44, which are involved in osteoclast migration and fusion (31-33), were also decreased in Cx37 deficient cultures. On the other hand, other molecules associated with osteoclast function were either not changed (osteoclast-associated receptor, OSCAR) or their decrease did not reach significance (integrin β3 and E-cadherin).

Recent evidence indicates that the Notch signaling pathway negatively modulates osteoclast differentiation (34;35). We therefore, investigated whether deleting Cx37 altered regulation of Notch signaling. Freshly isolated Cx37-deficient non-adherent bone marrow cells expressed higher levels of the Notch1-3 receptors compared to wild type cells, whereas the expression of the Notch target gene Hey-1 was unchanged (Fig. 8a). Moreover, the number of viable cells in cultures treated with M-CSF for 24h was significantly higher in $Cx37^{-/-}$ cells, and this difference disappeared when the cultures were treated with a Notch inhibitor (Fig. 8b). Increased expression of the Notch target Hey-1 was detected in mature osteoclasts and in whole bone lysates, whereas the levels of the receptors Notch1-3 were either unchanged or slightly increased. This evidence suggests that elevation of Notch signaling pathway in the absence of Cx37 contributes to the inhibition of osteoclastogenesis in $Cx37^{-/-}$ mice.

Ex vivo cultures of adherent bone marrow cells maintained in the presence of ascorbic acid and β-glycerophophate to induce osteoblast differentiation showed no difference in calcium deposition, a marker for mineralizing activity, between cells isolated from $Cx37^{-/-}$ and $Cx37^{+/+}$ controls (Fig. 9a). Moreover, the expression of the osteoblastic genes osteocalcin, alkaline phosphatase, collagen type 1a1, and bone sialoprotein was not affected by Cx37 deletion in the osteoblastic cells derived from adherent bone marrow cells (Fig. 9a) or in whole lumbar vertebra lysates (Fig. 9b). Similarly, no differences were seen in the level of mineralization on the vertebral bone in 2.5- and 5-month-old mice.

DISCUSSION

In this report, we describe the skeletal phenotype of mice with global deletion of Cx37, a member of the connexin family of proteins with previously unrecognized functions in bone cells. Cx37 is expressed in whole bone at levels about 4-fold lower than Cx43. Osteoblasts, osteocytes and osteoclasts all express Cx37, albeit at 60-400 fold lower levels than Cx43. We found that the skeletal phenotype of mice with global deletion of the gene results from an osteoclast cell-autonomous defect. Although non-adherent bone marrow cells express higher levels of markers of osteoclast precursors, their ability to become mature osteoclasts is impaired. This evidence, together with the decrease in osteoclast parameters *in vivo*, suggests that the increased bone mass and volume observed in $Cx37^{-/-}$ mice is due to defective osteoclast maturation and the consequent decreased osteoclast bone resorbing activity. Whether

decreased osteoclastogenesis in the absence of Cx37 is due to lack of cell-to-cell-communication, reduced communication with the extracellular medium through Cx37 hemichannels, or to defective Cx37-protein association independent of channel function, will be investigated in future studies.

Similar to our *in vivo* results, treatment of osteoclast precursors with agents that disassemble connexin channels leads to decreased osteoclast differentiation *in vitro*, with reduced fusion of osteoclast precursors compared to vehicle treated cultures (36-38). GAP27, a peptide that inhibits the function of the channel/hemichannel formed by Cx43 or Cx37, has been shown to block osteoclast differentiation (39;40). This decrease in osteoclastogenesis was attributed to reduced Cx43 function, since this was the only connexin protein described in osteoclastic cells. Our data, however, shows that Cx37 expression is required for osteoclast differentiation and the regulation of bone mass. A preliminary study presented in abstract form indicates that osteoclast-specific deletion of Cx43 has a similar impact on osteoclastogenesis as the absence of Cx37 (41). This raises the possibility that channels formed by both connexins (heteromeric) or docking of different channels each formed by one connexin are required for osteoclast maturation. The co-localization of Cx43 and Cx37 in heteromeric channels may not only alter channel properties, but also affect the interaction of the connexins with intracellular signaling molecules. On the other hand, expression of Cx43, but not Cx37, in osteoblast precursors is required for full osteoblast differentiation and for normal ossification of the developing embryos (42), suggesting that in osteoblastic cells the two connexins do not interact, and that Cx43 is the main connexin active in these cells.

Preliminary mechanistic studies show that cells lacking Cx37 exhibit increased Notch signaling activation in response to pro-osteoclastogenic stimuli, whereas in mature osteoclasts, Notch1-3 mRNA levels were normal. Furthermore, the number of viable cells is higher in non-adherent bone marrow cells treated with M-CSF, but returns to wild type control levels by inhibition of Notch signaling. The increase in cell number could be due to higher proliferation or reduced apoptosis. Enhanced proliferation of $Cx37^{-/-}$ osteoclast progenitor cells is supported by evidence showing that Cx37 suppresses the proliferation of rat insulinoma cells (43;44). Our data, however, contrast with evidence showing that deletion of Notch1-3 in osteoclast precursors using LysM-Cre (35), leads to an increase in proliferation. This discrepancy could be due to changes in other genes in the absence of Cx37, or to the temporal pre-osteoclast-specific elevation of Notch1-3 signaling in our studies. The expression of the Notch signaling target Hey-1 is highly increased in mature osteoclasts from Cx37-deficient mice, consistent with evidence that the Notch/RBPJk signaling pathway inhibits osteoclast differentiation (34;35). Further studies are required to establish the mechanism by which Cx37 modulates cell number and osteoclast differentiation through the Notch signaling pathway.

The absence of Cx37 in osteoblasts does not appear to alter the ability of these cells to synthesize bone matrix. However, our preliminary studies show that MLO-Y4 osteocytic cells in which the expression of Cx37 has been silenced using shRNA exhibit reduced RANKL/OPG ratio (not shown), which could contribute to reduced osteoclast formation. This contrasts with the effect of deletion of Cx43 from osteocytic cells, which results in higher RANKL/OPG ratio and increased osteoclastic bone resorption on endocortical bone surfaces (20;45). Cell-specific deletion of the Cx37 will be required to determine whether changes in osteoclastogenic cytokines expressed by osteocytes contribute to increased bone mass in $Cx37^{-/-}$ mice.

The phenotype of $Cx37^{-/-}$ mice is more pronounced in males than in females. Although the reasons for this sexual dimorphic skeletal phenotype are not known, the milder phenotype observed in female mice could be due to altered sex steroid levels secondary to the deficient oocyte maturation and abnormal corpora lutea previously reported (14). We confirmed the absence of terminally differentiated oocytes in our female $Cx37^{-/-}$ mice (**Fig. 10**). More osteoclasts resulting from lower circulating estrogens could counteract the decreased osteoclasts induced by Cx37

deficiency in female mice. Remarkably, a similar gender-specific effect has been recently found in a polymorphism of the Cx37 gene associated with decreased bone mass in males, but not in females in a Japanese population (13). This suggests that the presence of androgen, rather than changes in estrogen levels, is required for the effect of Cx37 deletion in bone. Future work will explore the potential interaction between estrogen and androgen with Cx37.

Deletion of Cx37 has a more profound effect at 2-2.5-month of age than in 5-month-old mice. This is evidenced by a higher bone volume and lower osteoclast and eroded surface in the vertebral bone of younger $Cx37^{-/-}$ animals compared to wild-type. Together with the fact that the difference in spinal BMD between the 2 genotypes is maintained throughout the study, this evidence suggests that deletion of Cx37 has a greater impact in the developing skeleton and is maintained into adulthood in the spine. The consistent response at the vertebra is contrasted with that at the long bones, where the phenotype existed across the age-span when assessed by DEXA, but only at the younger aged animals when trabecular bone was measured using μCT. The reason for the absence of effect in the distal femur (and the proximal tibia, not shown) at 5 months is not clear and warrants further investigation.

The higher effect of Cx37 removal on bone mineral density and bone volume in the cancellous bone and, in particular, in the axial skeleton contrasts with deletion of Cx43 from osteoblasts/osteocytes, in which the main effect is geometrical changes in cortical bone (20;45;46). Although Cx37 and Cx43 belong to the same α-family of connexins, their channels differ markedly in unitary conductance, pore diameter, specificity of ion permeability, and, potentially, ability to bind intracellular molecules (47). The two connexins are co-expressed in several tissues, but with different cellular specificity, expression levels, and function. Thus, the connexins exert opposing effects on rat insulinoma cell cycle progression; Cx37 increases the percentage of cells in G0/G1 and decreases the percentage of cells in S-phase, whereas Cx43 decreases the percentage of cells in G0/G1 and increases the percentage in S-phase (43). In addition, Cx43, but not Cx37, is able to confer responsiveness to bisphosphonates in connexin-deficient HeLa cells (48). In the female reproductive tissue, Cx43 is expressed in granulosa cells and Cx37 is mainly expressed in oocytes, and the expression of both connexins is required for full oocyte maturation. Interestingly, ectopic expression of Cx43 in oocytes can rescue the effect of Cx37 deletion, suggesting that Cx43 can exert the same functions than Cx37 in oocytes (49). However, this is not the case in osteoclasts, where Cx43 is highly expressed but cannot compensate for the lack of Cx37.

Femora from $Cx37^{-/-}$ mice exhibit tendencies towards a decrease in total bone area and towards an increase in marrow cavity area. Although these differences do not reach significance, the combination of these changes results in a significant decreased cortical thickness. Reduced cortical thickness could lead to lower mechanical strength. However, femora from $Cx37^{-/-}$ mice are stronger, as evidenced by higher ultimate force and stiffness. This suggests that deletion of Cx37 results in changes in the bone matrix composition, likely the organic phase since it primarily dictates toughness while the mineral phase dictates modulus, leading to improved bone strength. On the other hand, deletion of Cx43 from mature osteoblasts/osteocytes or only from osteocytes does not change ultimate force or stiffness, but results in reduced bone material properties (Young's modulus and ultimate stress) (50). Similarly, expression of a Cx43 mutant associated with occulodentodigital dysplasia results in defective material properties (51). This evidence suggests that Cx43 and Cx37 have different effects on mature osteoblasts/osteocytes synthetic activity or the ability of the cells to maintain the extracellular matrix in cortical bone. Future studies are required to determine the nature of the changes induced by Cx37 deletion on the bone material.

In summary, our studies show that Cx37 expression in osteoclast precursors is required for osteoclast differentiation and full maturation. Lack of Cx37 leads to a sustained increased in bone mass, in particular in the axial skeleton. Our findings demonstrate that Cx37 modulates osteoclast differentiation and therefore could be

targeted to reduce osteoclastic bone resorption. Inhibition of connexin function *in vivo* has been tested using mimetic peptides, which block connexin channels (52). This approach has been successful in preventing alterations in blood-brain barrier permeability and spinal cord injury (53;54), raising the possibility that these mimetic peptides could be used to target specifically osteoclast precursors leading to reduced bone resorption and maintenance of bone mass.

REFERENCES

1. Plotkin, L. I. and Bellido, T. (2013) Beyond gap junctions: Connexin43 and bone cell signaling. *Bone* **52,** 157-166
2. Nielsen, M. S., Nygaard, A. L., Sorgen, P. L., Verma, V., Delmar, M., and Holstein-Rathlou, N. H. (2012) Gap junctions. *Compr. Physiol* **2,** 1981-2035
3. Herve, J. C., Derangeon, M., Sarrouilhe, D., Giepmans, B. N., and Bourmeyster, N. (2011) Gap junctional channels are parts of multiprotein complexes. *Biochim. Biophys Acta* **1818,** 1844-1865
4. Segretain, D. and Falk, M. M. (2004) Regulation of connexin biosynthesis, assembly, gap junction formation, and removal. *Biochim. Biophys. Acta* **1662,** 3-21
5. White, T. W., Paul, D. L., Goodenough, D. A., and Bruzzone, R. (1995) Functional analysis of selective interactions among rodent connexins. *Mol. Biol. Cell* **6,** 459-470
6. Paic, F., Igwe, J. C., Nori, R., Kronenberg, M. S., Franceschetti, T., Harrington, P., Kuo, L., Shin, D. G., Rowe, D. W., Harris, S. E., and Kalajzic, I. (2009) Identification of differentially expressed genes between osteoblasts and osteocytes. *Bone* **45,** 682-692
7. Sohl, G. and Willecke, K. (2004) Gap junctions and the connexin protein family. *Cardiovasc. Res.* **62,** 228-232
8. Chanson, M. and Kwak, B. R. (2007) Connexin37: a potential modifier gene of inflammatory disease. *J. Mol. Med. (Berl)* **85,** 787-795
9. Hanner, F., Sorensen, C. M., Holstein-Rathlou, N. H., and Peti-Peterdi, J. (2010) Connexins and the kidney. *Am. J. Physiol Regul. Integr. Comp Physiol* **298,** R1143-R1155
10. Figueroa, X. F. and Duling, B. R. (2009) Gap junctions in the control of vascular function. *Antioxid. Redox. Signal.* **11,** 251-266
11. Simon, A. M. and McWhorter, A. R. (2002) Vascular abnormalities in mice lacking the endothelial gap junction proteins connexin37 and connexin40. *Dev. Biol.* **251,** 206-220
12. Morel, S., Burnier, L., Roatti, A., Chassot, A., Roth, I., Sutter, E., Galan, K., Pfenniger, A., Chanson, M., and Kwak, B. R. (2010) Unexpected role for the human Cx37 C1019T polymorphism in tumour cell proliferation. *Carcinogenesis* **31,** 1922-1931
13. Yamada, Y., Ando, F., and Shimokata, H. (2007) Association of candidate gene polymorphisms with bone mineral density in community-dwelling Japanese women and men. *Int. J. Mol. Med.* **19,** 791-801
14. Simon, A. M., Goodenough, D. A., Li, E., and Paul, D. L. (1997) Female infertility in mice lacking connexin 37. *Nature* **385,** 525-529
15. Kalajzic, I., Braut, A., Guo, D., Jiang, X., Kronenberg, M. S., Mina, M., Harris, M. A., Harris, S. E., and Rowe, D. W. (2004) Dentin matrix protein 1 expression during osteoblastic differentiation, generation of an osteocyte GFP-transgene. *Bone* **35,** 74-82
16. Rhee, Y., Allen, M. R., Condon, K., Lezcano, V., Ronda, A. C., Galli, C., Olivos, N., Passeri, G., O'Brien, C. A., Bivi, N., Plotkin, L. I., and Bellido, T. (2011) PTH receptor signaling in osteocytes governs periosteal bone formation and intra-cortical remodeling. *J. Bone Miner. Res.* **26,** 1035-1046
17. Bivi, N., Lezcano, V., Romanello, M., Bellido, T., and Plotkin, L. I. (2011) Connexin43 interacts with βarrestin: a pre-requisite for osteoblast survival induced by parathyroid hormone. *J. Cell. Biochem.* **112,** 2920-2930

18. Plotkin, L. I., Weinstein, R. S., Parfitt, A. M., Roberson, P. K., Manolagas, S. C., and Bellido, T. (1999) Prevention of osteocyte and osteoblast apoptosis by bisphosphonates and calcitonin. *J. Clin. Invest.* **104,** 1363-1374
19. Thi, M. M., Urban-Maldonado, M., Spray, D. C., and Suadicani, S. O. (2010) Characterization of human telomerase reverse transcriptase (hTERT) immortalized osteoblast cell lines generated from wildtype and connexin43-null mouse calvaria. *Am. J Physiol Cell Physiol* **299,** C994-C1006
20. Bivi, N., Condon, K. W., Allen, M. R., Farlow, N., Passeri, G., Brun, L., Rhee, Y., Bellido, T., and Plotkin, L. I. (2012) Cell autonomous requirement of connexin 43 for osteocyte survival: consequences for endocortical resorption and periosteal bone formation. *J. Bone Min. Res.* **27,** 374-389
21. Bivi, N., Bereszczak, J. Z., Romanello, M., Zeef, L. A., Delneri, D., Quadrifoglio, F., Moro, L., Brancia, F. L., and Tell, G. (2009) Transcriptome and proteome analysis of osteocytes treated with nitrogen-containing bisphosphonates. *J. Proteome. Res.* **8,** 1131-1142
22. Niranjan, T., Bielesz, B., Gruenwald, A., Ponda, M. P., Kopp, J. B., Thomas, D. B., and Susztak, K. (2008) The Notch pathway in podocytes plays a role in the development of glomerular disease. *Nat. Med.* **14,** 290-298
23. Albers, J., Keller, J., Baranowsky, A., Beil, F. T., Catala-Lehnen, P., Schulze, J., Amling, M., and Schinke, T. (2013) Canonical Wnt signaling inhibits osteoclastogenesis independent of osteoprotegerin. *J Cell Biol.* **200,** 537-549
24. Rodriguez, S., Chora, A., Goumnerov, B., Mumaw, C., Goebel, W. S., Fernandez, L., Baydoun, H., HogenEsch, H., Dombkowski, D. M., Karlewicz, C. A., Rice, S., Rahme, L. G., and Carlesso, N. (2009) Dysfunctional expansion of hematopoietic stem cells and block of myeloid differentiation in lethal sepsis. *Blood* **114,** 4064-4076
25. Tu, X., Joeng, K. S., Nakayama, K. I., Nakayama, K., Rajagopal, J., Carroll, T. J., McMahon, A. P., and Long, F. (2007) Noncanonical Wnt signaling through G protein-linked PKCdelta activation promotes bone formation. *Dev. Cell* **12,** 113-127
26. Bivi, N., Pacheco-Costa, R., Brun, L. R., Murphy, T. R., Farlow, N. R., Robling, A. G., Bellido, T., and Plotkin, L. I. (2013) Absence of Cx43 selectively from osteocytes enhances responsiveness to mechanical force in mice. *J. Orthop. Res.* **31,** 1075-1081
27. Dempster, D. W., Compston, J. E., Drezner, M. K., Glorieux, F. H., Kanis, J. A., Malluche, H., Meunier, P. J., Ott, S. M., Recker, R. R., and Parfitt, A. M. (2013) Standardized nomenclature, symbols, and units for bone histomorphometry: A 2012 update of the report of the ASBMR Histomorphometry Nomenclature Committee. *J. Bone Miner. Res.* **28,** 2-17
28. Plotkin, L. I., Bivi, N., and Bellido, T. (2011) A bisphosphonate that does not affect osteoclasts prevents osteoblast and osteocyte apoptosis and the loss of bone strength induced by glucocorticoids in mice. *Bone* **49,** 122-127
29. Allen, M. R., Reinwald, S., and Burr, D. B. (2008) Alendronate reduces bone toughness of ribs without significantly increasing microdamage accumulation in dogs following 3 years of daily treatment. *Calcif. Tissue Int.* **82,** 354-360
30. Takayanagi, H., Kim, S., Koga, T., Nishina, H., Isshiki, M., Yoshida, H., Saiura, A., Isobe, M., Yokochi, T., Inoue, J., Wagner, E. F., Mak, T. W., Kodama, T., and Taniguchi, T. (2002) Induction and activation of the transcription factor NFATc1 (NFAT2) integrate RANKL signaling in terminal differentiation of osteoclasts. *Dev. Cell* **3,** 889-901
31. Kania, J. R., Kehat-Stadler, T., and Kupfer, S. R. (1997) CD44 antibodies inhibit osteoclast formation. *J. Bone Miner. Res.* **12,** 1155-1164
32. Cackowski, F. C., Anderson, J. L., Patrene, K. D., Choksi, R. J., Shapiro, S. D., Windle, J. J., Blair, H. C., and Roodman, G. D. (2009) Osteoclasts are important for bone angiogenesis. *Blood* **115,** 140-149
33. MacLauchlan, S., Skokos, E. A., Meznarich, N., Zhu, D. H., Raoof, S., Shipley, J. M., Senior, R. M., Bornstein, P., and Kyriakides, T. R. (2009) Macrophage fusion, giant cell formation, and the foreign body response require matrix metalloproteinase 9. *J. Leukoc. Biol.* **85,** 617-626

34. Ma, J., Liu, Y. L., Hu, Y. Y., Wei, Y. N., Zhao, X. C., Dong, G. Y., Qin, H. Y., Ding, Y., and Han, H. (2013) Disruption of the transcription factor RBP-J results in osteopenia attributable to attenuated osteoclast differentiation. *Mol. Biol. Rep.* **40,** 2097-2105
35. Bai, S., Kopan, R., Zou, W., Hilton, M. J., Ong, C. T., Long, F., Ross, F. P., and Teitelbaum, S. L. (2008) NOTCH1 regulates osteoclastogenesis directly in osteoclast precursors and indirectly via osteoblast lineage cells. *J. Biol. Chem.* **283,** 6509-6518
36. Ilvesaro, J. and Tuukkanen, J. (2003) Gap-junctional regulation of osteoclast function. *Crit Rev. Eukaryot. Gene Expr.* **13,** 133-146
37. Matemba, S. F., Lie, A., and Ransjo, M. (2006) Regulation of osteoclastogenesis by gap junction communication. *J. Cell Biochem.* **99,** 528-537
38. Schilling, A. F., Filke, S., Lange, T., Gebauer, M., Brink, S., Baranowsky, A., Zustin, J., and Amling, M. (2008) Gap junctional communication in human osteoclasts in vitro and in vivo. *J. Cell Mol. Med.* **12,** 2497-2504
39. Ilvesaro, J., Tavi, P., and Tuukkanen, J. (2001) Connexin-mimetic peptide Gap 27 decreases osteoclastic activity. *BMC. Musculoskelet. Disord.* **2,** 10
40. Kylmaoja, E., Kokkonen, H., Kauppinen, K., Hussar, P., Sato, T., Haugan, K., Larsen, B. D., and Tuukkanen, J. (2013) Osteoclastogenesis is influenced by modulation of gap junctional communication with antiarrhythmic peptides. *Calcif. Tissue Int.* **92,** 270-281
41. Sternlieb, M., Paul, E., Donahue, H. J., and Zhang.Y. (2012) Ablation of connexin 43 in osteoclasts leads to decreased in vivo osteoclastogenesis. *J. Bone Miner. Res.* **27,** S53
42. Lecanda, F., Warlow, P. M., Sheikh, S., Furlan, F., Steinberg, T. H., and Civitelli, R. (2000) Connexin43 deficiency causes delayed ossification, craniofacial abnormalities, and osteoblast dysfunction. *J. Cell Biol.* **151,** 931-944
43. Burt, J. M., Nelson, T. K., Simon, A. M., and Fang, J. S. (2008) Connexin 37 profoundly slows cell cycle progression in rat insulinoma cells. *Am. J. Physiol Cell Physiol* **295,** C1103-C1112
44. Nelson, T. K., Sorgen, P. L., and Burt, J. M. (2013) Carboxy terminus and pore-forming domain properties specific to Cx37 are necessary for Cx37-mediated suppression of insulinoma cell proliferation. *Am. J. Physiol Cell Physiol* **305,** C1246-C1256
45. Zhang, Y., Paul, E. M., Sathyendra, V., Davidson, A., Bronson, S., Srinivasan, S., Gross, T. S., and Donahue, H. J. (2011) Enhanced osteoclastic resorption and responsiveness to mechanical load in gap junction deficient bone. *PLoS ONE* **6,** e23516
46. Watkins, M., Grimston, S. K., Norris, J. Y., Guillotin, B., Shaw, A., Beniash, E., and Civitelli, R. (2011) Osteoblast Connexin43 modulates skeletal architecture by regulating both arms of bone remodeling. *Mol. Biol. Cell* **22,** 1240-1251
47. Ek-Vitorin, J. F. and Burt, J. M. (2013) Structural basis for the selective permeability of channels made of communicating junction proteins. *Biochim. Biophys. Acta* **1828,** 51-68
48. Plotkin, L. I., Manolagas, S. C., and Bellido, T. (2002) Transduction of cell survival signals by connexin-43 hemichannels. *J. Biol. Chem.* **277,** 8648-8657
49. Li, T. Y., Colley, D., Barr, K. J., Yee, S. P., and Kidder, G. M. (2007) Rescue of oogenesis in Cx37-null mutant mice by oocyte-specific replacement with Cx43. *J. Cell Sci.* **120,** 4117-4125
50. Bivi, N., Nelson, M. T., Faillace, M. E., Li, J., Miller, L. M., and Plotkin, L. I. (2012) Deletion of Cx43 from osteocytes results in defective bone material properties but does not decrease extrinsic strength in cortical bone. *Calcif. Tissue Int.* **91,** 215-224
51. Zappitelli, T., Chen, F., Moreno, L., Zirngibl, R. A., Grynpas, M., Henderson, J. E., and Aubin, J. E. (2013) The G60S Connexin 43 Mutation Activates the Osteoblast Lineage and Results in a Resorption-Stimulating Bone Matrix and Abrogation of old Age-related Bone Loss. *J. Bone Miner. Res.* **28,** 2400-2413
52. Evans, W. H. and Leybaert, L. (2007) Mimetic peptides as blockers of connexin channel-facilitated intercellular communication. *Cell Commun. Adhes.* **14,** 265-273

53. O'Carroll, S. J., Gorrie, C. A., Velamoor, S., Green, C. R., and Nicholson, L. F. (2013) Connexin43 mimetic peptide is neuroprotective and improves function following spinal cord injury. *Neurosci. Res.* **75,** 256-267
54. De Bock, M., Culot, M., Wang, N., Bol, M., Decrock, E., De Vuyst, E., da Costa, A., Dauwe, I., Vinken, M., Simon, A. M., Rogiers, V., De Ley, G., Evans, W. H., Bultynck, G., Dupont, G., Cecchelli, R., and Leybaert, L. (2011) Connexin channels provide a target to manipulate brain endothelial calcium dynamics and blood-brain barrier permeability. *J. Cereb. Blood Flow Metab* **31,** 1942-1957

Acknowledgements - The authors thank Surajudeen Bolarinwa, Meloney Cregor, Drew M. Brown, Huajia Zhang, and Anthony Acton Jr. for technical assistance. We are grateful to Dr. Teresita Bellido for helpful discussions and critical reading of the manuscript, to Dr. Nadia Carlesso for the FACS analysis, and to Dr. Munro Peacock for the measurement of circulating alkaline phosphatase.

FOOTNOTES

*This work was supported by NIH grant R01-AR053643 (to LIP), CTSI PDT Grant TR000006 from IU (to LIP and MRA). RPC received a scholarship from CAPES, Brazil (1065/11-4), and IH received scholarships from Ronald E. McNair Post-baccalaureate Achievement Program from the U.S. Department of Education (2012) and CTSI-Clinical and Transitional Sciences Institute Award (2013). μCT studies were performed using equipment obtained with the NIH grant S10-RR023710 (PI: James Williams, Department of Anatomy and Cell Biology, Indiana University School of Medicine).

To whom correspondence should be addressed: Lilian I. Plotkin, Ph.D. Department of Anatomy and Cell Biology Indiana University School of Medicine 635 Barnhill Drive, MS-5035 Indianapolis, IN, USA, Tel: 317-274-5317; Fax: 317-278-2040; e-mail: lplotkin@iupui.edu

[1]The abbreviations used are: ATP6v0d2, d2 isoform of vacuolar ATPase V_o domain; BFR/BS, bone formation rate; BMD, bone mineral density; CTX, C-telopeptide fragments of type I collagen; Cx, connexin; DCSTAMP, dendritic cell-specific transmembrane protein; ES/BS, eroded surface; FBS, fetal bovine serum; KOH, Potassium hydroxide; MMP9, matrix metalloproteinase; M-CSF, Macrophage colony-stimulating factor; MS/BS, Mineralizing surface; MAR, mineral apposition rate; NFATc1, nuclear factor of activated T-cells; NOc/BS, osteoclast number; NOb/BS, number of osteoblasts; ObS/BS, surface covered by osteoblasts; OcS/BS, surface covered by osteoclasts; QS/BS, quiescent surface; RANK, Receptor activator of nuclear factor kappa-B ligand; RANKL, receptor activator of nuclear factor kappa-B ligand; TRAP, tartrate-resistant acid phosphatase.

LEGENDS

FIGURE 1. Cx37 is expressed in all bone cells, although at lower levels than Cx43.
Cx37 and Cx43 mRNA expression measured by qPCR and corrected by GAPDH in murine lumbar vertebra, OB-6 and immortalized calvaria osteoblastic cells, and MLO-Y4 osteocytic cells (**a**); and in osteoblasts and osteocytes isolated from murine calvaria, and in osteoclasts obtained *in vitro* by treatment of bone marrow non-adherent cells with M-CSF and sRANKL (**b**).

FIGURE 2. Global deletion of Cx37 increases bone mass.
(a) Representative images of whole body histological preparations stained by alcian blue/alizarin red in 5 day-old mice for evaluation of cartilage and calcified tissue. **(b)** Total body weight of male and female mice measured monthly from 2 to 5 months of age. Symbols correspond to mean ± SD, n=8-17. * $p<0.05$ versus $Cx37^{+/+}$ mice by t-test. (**c**) Total, spinal and femoral bone mineral density was assessed monthly by DEXA in $Cx37^{+/+}$ and $Cx37^{-/-}$ mice from 2 to 5 months of age. Symbols correspond to mean ± SD, n=8-17. * $p<0.05$ versus $Cx37^{+/+}$ mice by t-test.

FIGURE 3. **Global deletion of Cx37 results in high bone volume in cancellous bone.** μCT analysis of (**a**) cancellous bone microarchitecture in L6 vertebrae in 2.5-month-old mice (n=3-4) and L4 vertebrae in 5-month-old mice (n=7-8); (**b**) cancellous bone microarchitecture in the distal femur in 2.5-month-old mice (n=3-4) or 5-mont-old mice (n=9-11); and (**c**) cortical bone geometry in the femoral midshaft in 5-month-old mice (n=8-13). Bars are mean ± SD. * $p<0.05$ versus $Cx37^{+/+}$ mice by t-test. Representative images of vertebrae from wild type and $Cx37^{-/-}$ littermate controls are shown in (**a**).

FIGURE 4. Mice lacking Cx37 exhibit increased mechanical strength. Biomechanical properties were measured in vertebral bone (n=5-8) (**a**) and femoral midshaft (n=8-13) (**b**) by compression and 3-point bending testing, respectively. Estimates of material properties were derived for the femoral midshaft. Bars are mean ± SD. * $p<0.05$ versus $Cx37^{+/+}$ mice by t-test.

FIGURE 5. Removal of Cx37 decreases osteoclast number in mice. Static and dynamic histomorphometric parameters were scored in lumbar vertebra bone sections of 2.5- **(a)** and 5- **(b)** month-old $Cx37^{+/+}$ and $Cx37^{-/-}$ male mice. (**a** and **b**) Osteoclast number (NOc/BS), surface covered by osteoclasts (OcS/BS), eroded surface (ES/BS), number of osteoblasts (NOb/BS), surface covered by osteoblasts (ObS/BS), quiescent surface (QS/BS), were measured in vertebral bone sections stained for TRAPase. Bars are mean ± SD, n=4. * $p<0.05$ versus $Cx37^{+/+}$ mice by t-test. Representative images of vertebral bone stained for mineralized bone (von Kossa tetrachrome, left) and osteoclasts (right) are shown. Scale bars correspond to 400 μm and 100 μm for von Kossa and TRAP images, respectively. Insets in the TRAP images show osteoclasts at higher magnification. Scale bars correspond to 50 μm. (**c**) Mineralizing surface (MS/BS), mineral apposition rate (MAR) and bone formation rate (BFR/BS) were measure in unstained sections of lumbar vertebra from 5-month-old mice. Bars are mean ± SD, n=4-5.

FIGURE 6. Circulating markers of bone formation and resorption are not altered in mice expressing or lacking Cx37. Circulating levels for CTX, alkaline phosphatase, osteocalcin, and sclerostin were measured in serum of $Cx37^{+/+}$ and $Cx37^{-/-}$ mice at the indicated ages. Bars are mean ± SD, n=4-11.

FIGURE 7. Deficient osteoclast differentiation and fusion in Cx37 knockout mice. (a) Gene expression in vertebral bone preparations from $Cx37^{+/+}$ and $Cx37^{-/-}$ littermates. mRNA relative levels were measured by qPCR and corrected by GAPDH. Bars are mean ± SD, n=4-10 mice/genotype. **(b)** Non-adherent cells isolated from individual animals were differentiated into osteoclasts by treatment with M-CSF and sRANKL for 5 days. Representative images of osteoclasts stained for TRAP are shown. Bar represents 400μm. Osteoclast number and size, and the number of nuclei/osteoclast were scored. Bars are mean ± SD, n=4 mice/genotype. **(c)** Dot blots show Gr1 and CD11b expression in a representative experiment. Numbers indicate percentage of cells positive for the marker of osteoclast precursors CD11b. Expression levels of CD11b, CD14 and RANK mRNA were measured in non-adherent bone marrow cells. mRNA relative levels were measured by qPCR and corrected by GAPDH. Bars are mean ± SD, n=4 mice/genotype. * $p<0.05$ versus $Cx37^{+/+}$ mice by t-test. **(d)** Gene expression was assessed in mature (differentiated) osteoclasts generated by treatment of bone marrow non-adherent cells with M-CSF/sRANKL. Genes associated with osteoclast maturation, function and fusion are shown. mRNA relative levels were measured by qPCR and corrected by GAPDH. Bars are mean ± SD, n=4 mice/genotype. * $p<0.05$ versus $Cx37^{+/+}$ mice by t-test.

FIGURE 8. Increased Notch signaling in osteoclasts derived from Cx37-deficient bone marrow cells. (a) Gene expression of non-adherent cells isolated from $Cx37^{+/+}$ and $Cx37^{-/-}$ littermates. mRNA relative levels were measured by qPCR and corrected by GAPDH. Bars are mean ± SD, n=3 mice/genotype. * $p<0.05$ versus $Cx37^{+/+}$ mice by t-test. (**b**) Cell viability was determined by MTT assay. Bars are mean ± SD, n=3 replicas for one mouse/genotype. * $p<0.05$ versus $Cx37^{+/+}$ mice by one-way-ANOVA. (**c**) Gene expression was assessed in mature (differentiated) osteoclasts generated by treatment of bone marrow non-adherent cells with M-CSF/sRANKL. Genes associated with Notch signaling are shown. mRNA relative levels were measured by qPCR and corrected by GAPDH. Bars are mean ± SD, n=3 mice/genotype. * $p<0.05$ versus $Cx37^{+/+}$ mice by t-test. (**d**) Expression of Notch receptors and Hey-1 in vertebral bone from $Cx37^{+/+}$ and $Cx37^{-/-}$ littermates. mRNA relative levels were measured by qPCR and corrected by GAPDH. Bars are mean ± SD, n=6-8 mice/genotype. * $p<0.05$ versus $Cx37^{+/+}$ mice by t-test.

FIGURE 9. **Deletion of Cx37 does not alter osteoblast differentiation.** (**a**) Adherent bone marrow cells

from $Cx37^{+/+}$ and $Cx37^{-/-}$ mice were cultured in the presence of ascorbic acid/β-glycerophosphate for 14 days. Representative images of cells stained with alizarin red, and mineralization assessed by optical density are shown. Relative mRNA expression of osteoblastic genes was measured by qPCR and corrected by GAPDH in these cultures. Bars are mean ± SD, n=4. (**b**) Gene expression in 6th lumbar vertebra from $Cx37^{+/+}$ and $Cx37^{-/-}$ mice measured by qPCR and corrected by GAPDH. Bars are mean ± SD, n=4.

Figure 10. Lack of full oocyte maturation in $Cx37^{-/-}$ mice. Representative images of ovarian sections stained with hematoxilin/eosin from $Cx37^{+/+}$ and $Cx37^{-/-}$ mice, showing the lack of terminally differentiated Graafian follicles in the Cx37 null mice. Arrows point at a Graafian follicle in the $Cx37^{+/+}$ mice ovary. Bars represent 200μm.

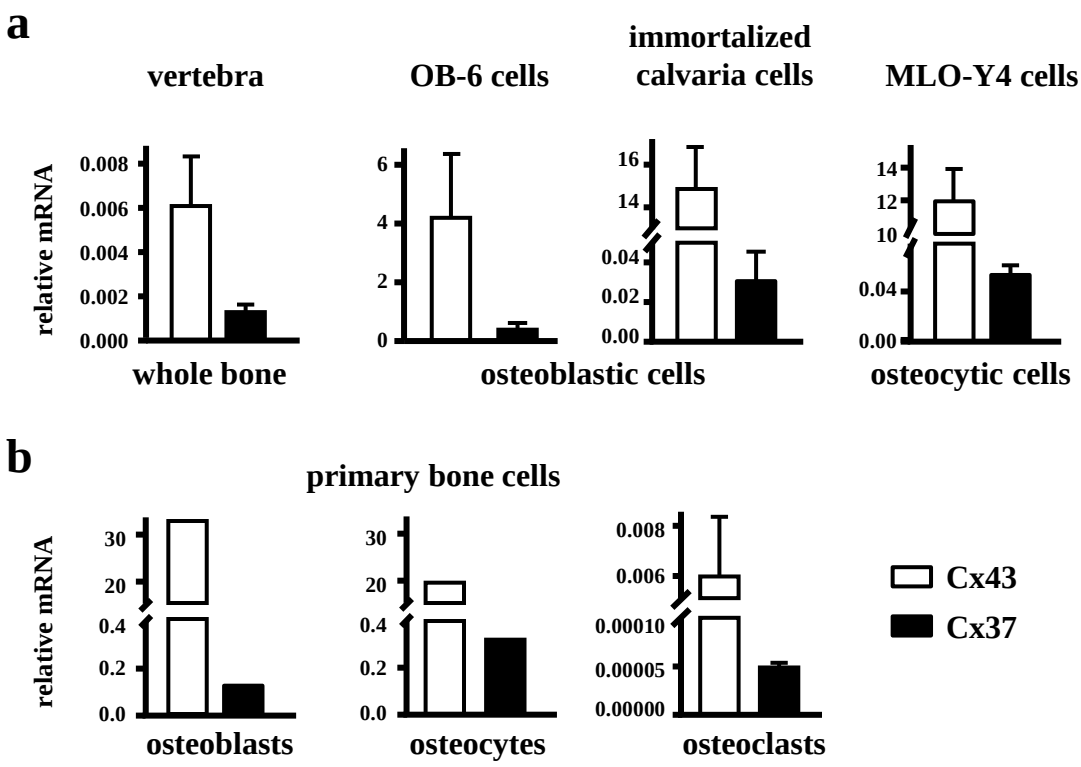
a
vertebra
OB-6 cells
immortalized calvaria cells
MLO-Y4 cells
relative mRNA
0.008
0.006
0.004
0.002
0.000
6
4
2
0
16
14
0.04
0.02
0.00
14
12
10
0.04
0.00
whole bone
osteoblastic cells
osteocytic cells
b
primary bone cells
relative mRNA
30
20
0.4
0.2
0.0
0.008
0.006
0.00010
0.00005
0.00000
Cx43
Cx37
osteoblasts
osteocytes
osteoclasts

Figure 1

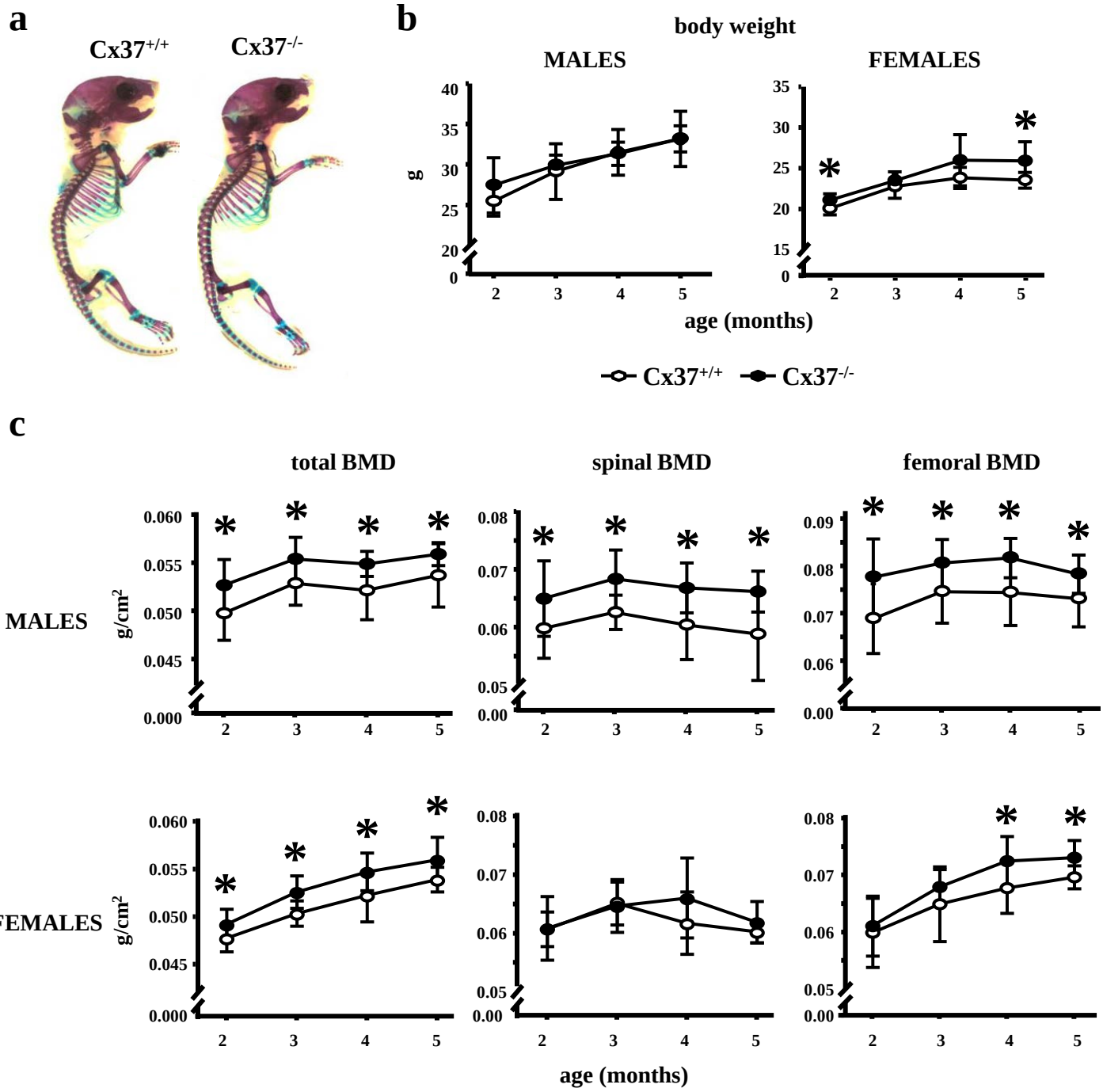
a
Cx37+/+
Cx37-/-
b
body weight
MALES
FEMALES
g
age (months)
Cx37+/+
Cx37-/-
c
total BMD
spinal BMD
femoral BMD
MALES
FEMALES
g/cm2
age (months)

Figure 2

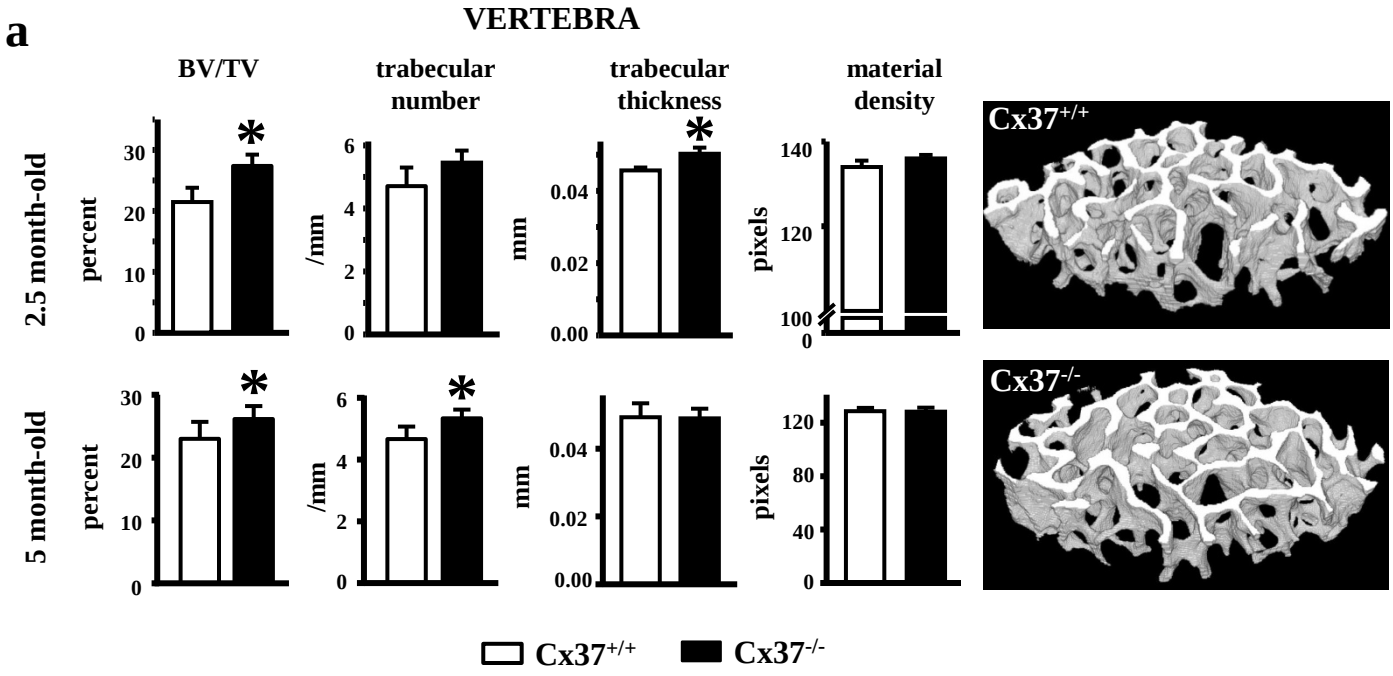
a
VERTEBRA
BV/TV
trabecular number
trabecular thickness
material density
2.5 month-old
5 month-old
percent
/mm
mm
pixels
Cx37+/+
Cx37-/-
Cx37+/+
Cx37-/-

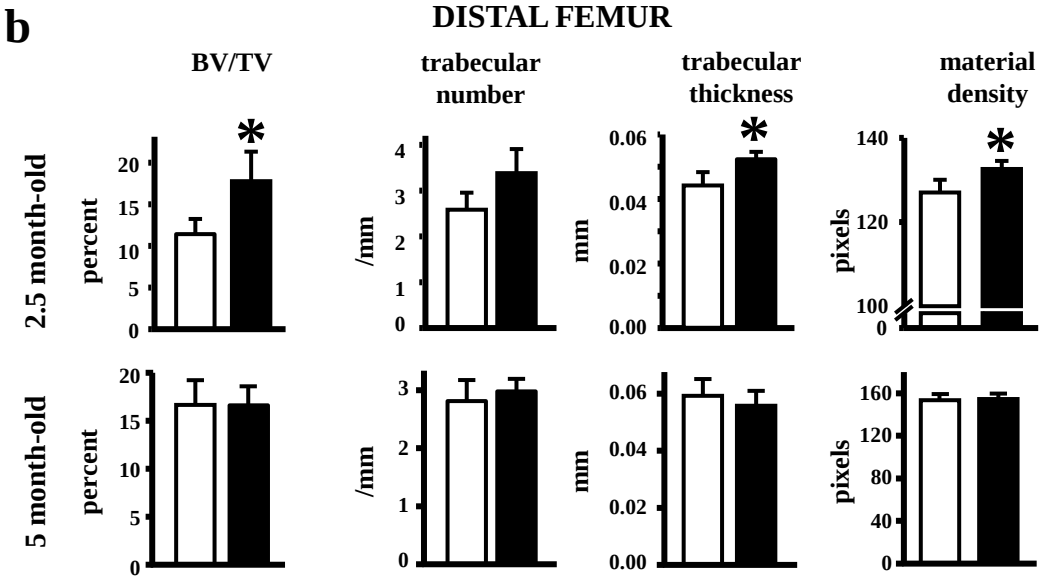
b
DISTAL FEMUR
BV/TV
trabecular number
trabecular thickness
material density
2.5 month-old
5 month-old
percent
/mm
mm
pixels

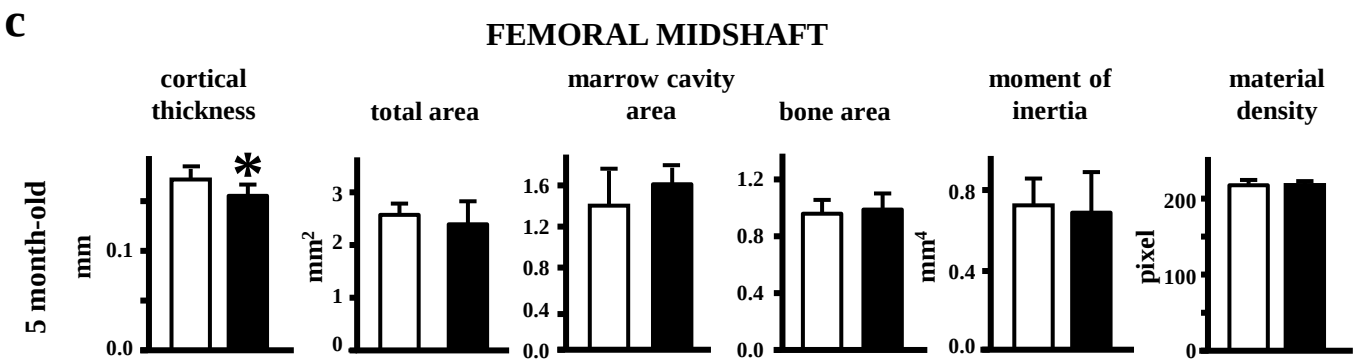
c
FEMORAL MIDSHAFT
cortical thickness
total area
marrow cavity area
bone area
moment of inertia
material density
5 month-old
mm
mm2
mm4
pixel

Figure 3

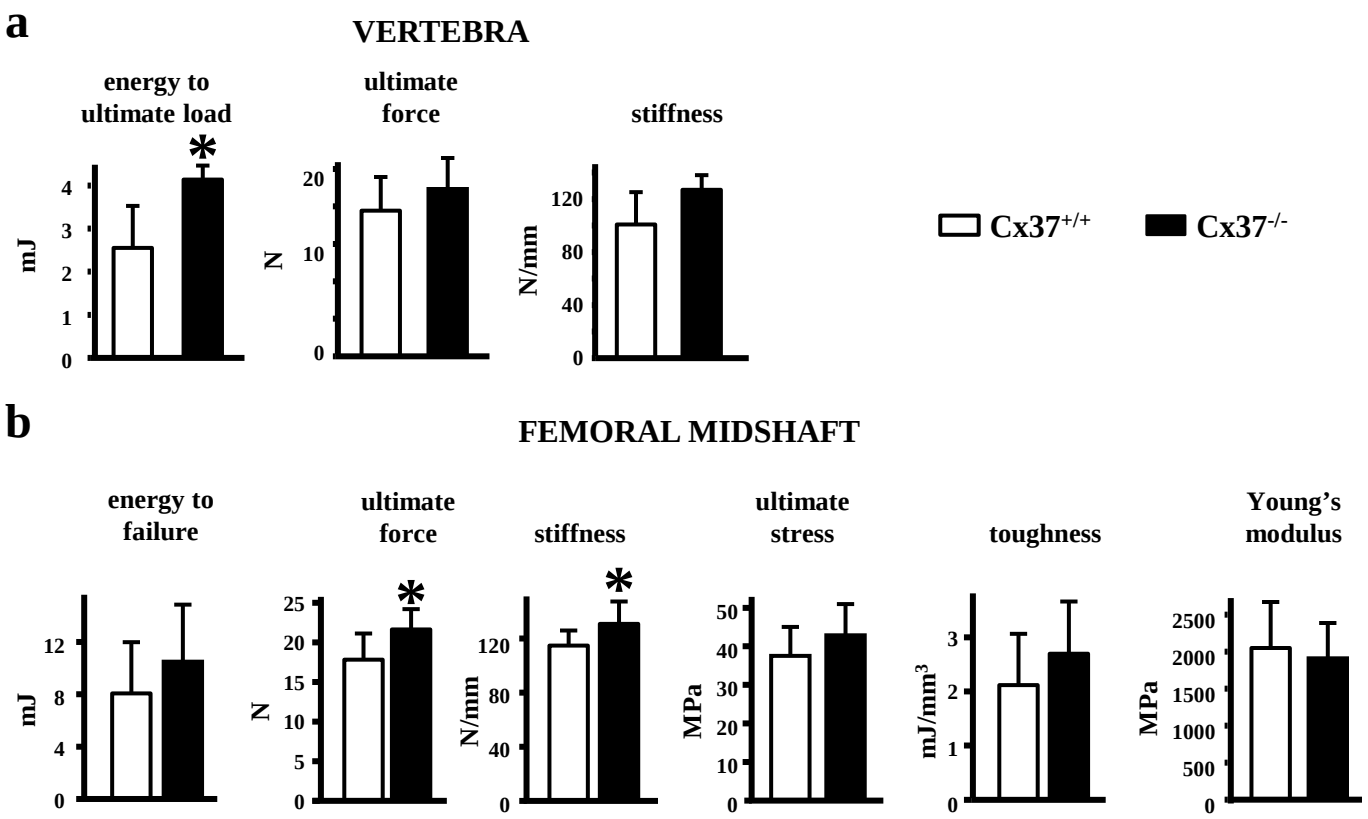
a
VERTEBRA
energy to ultimate load
ultimate force
stiffness
mJ
N
N/mm
Cx37+/+
Cx37-/-
b
FEMORAL MIDSHAFT
energy to failure
ultimate force
stiffness
ultimate stress
toughness
Young's modulus
mJ
N
N/mm
MPa
mJ/mm3
MPa

Figure 4

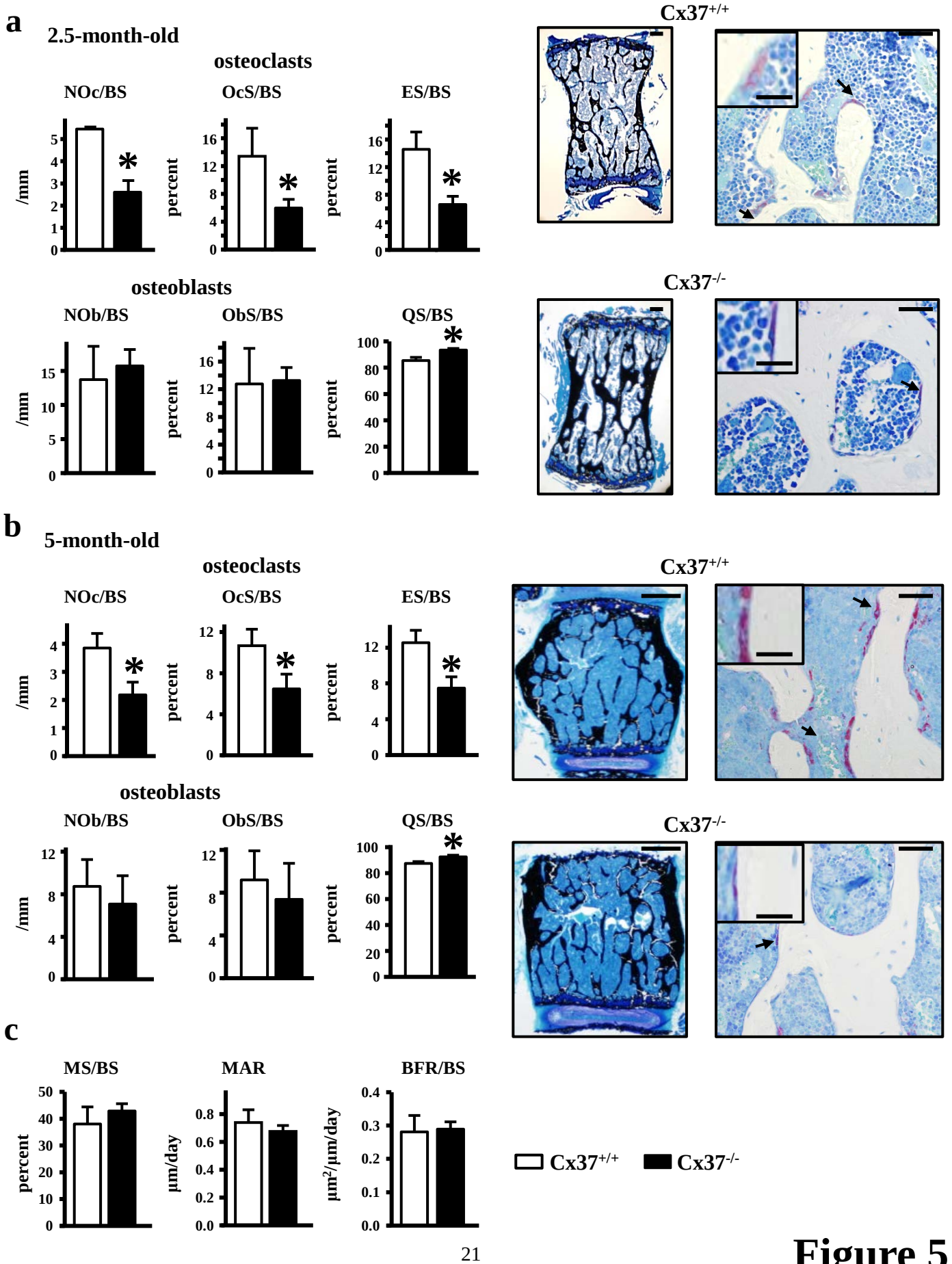
a
2.5-month-old
osteoclasts
NOc/BS
OcS/BS
ES/BS
/mm
percent
osteoblasts
NOb/BS
ObS/BS
QS/BS
Cx37+/+
Cx37-/-
b
5-month-old
c
MS/BS
MAR
BFR/BS
percent
µm/day
µm2/µm/day
Cx37+/+
Cx37-/-

Figure 5

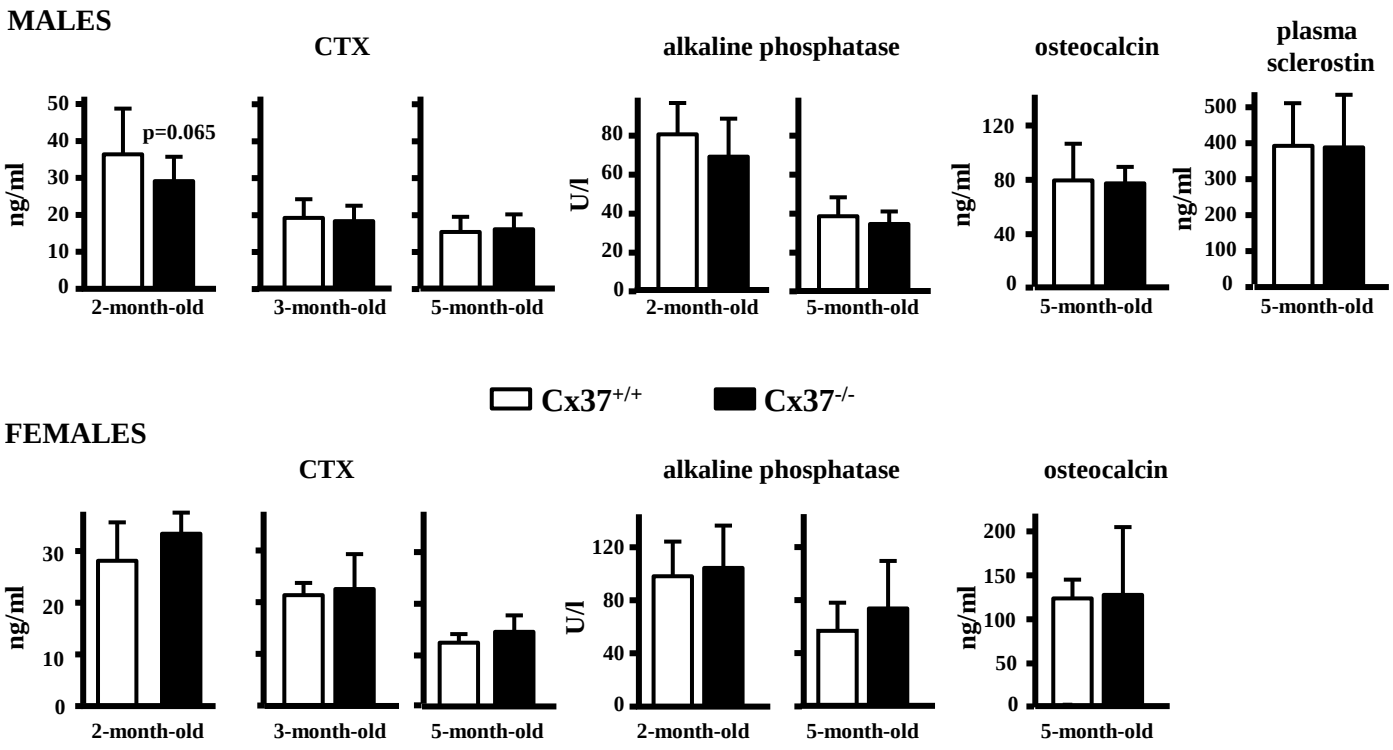
MALES
CTX
alkaline phosphatase
osteocalcin
plasma sclerostin
ng/ml
U/l
p=0.065
2-month-old
3-month-old
5-month-old
Cx37+/+
Cx37-/-
FEMALES

Figure 6

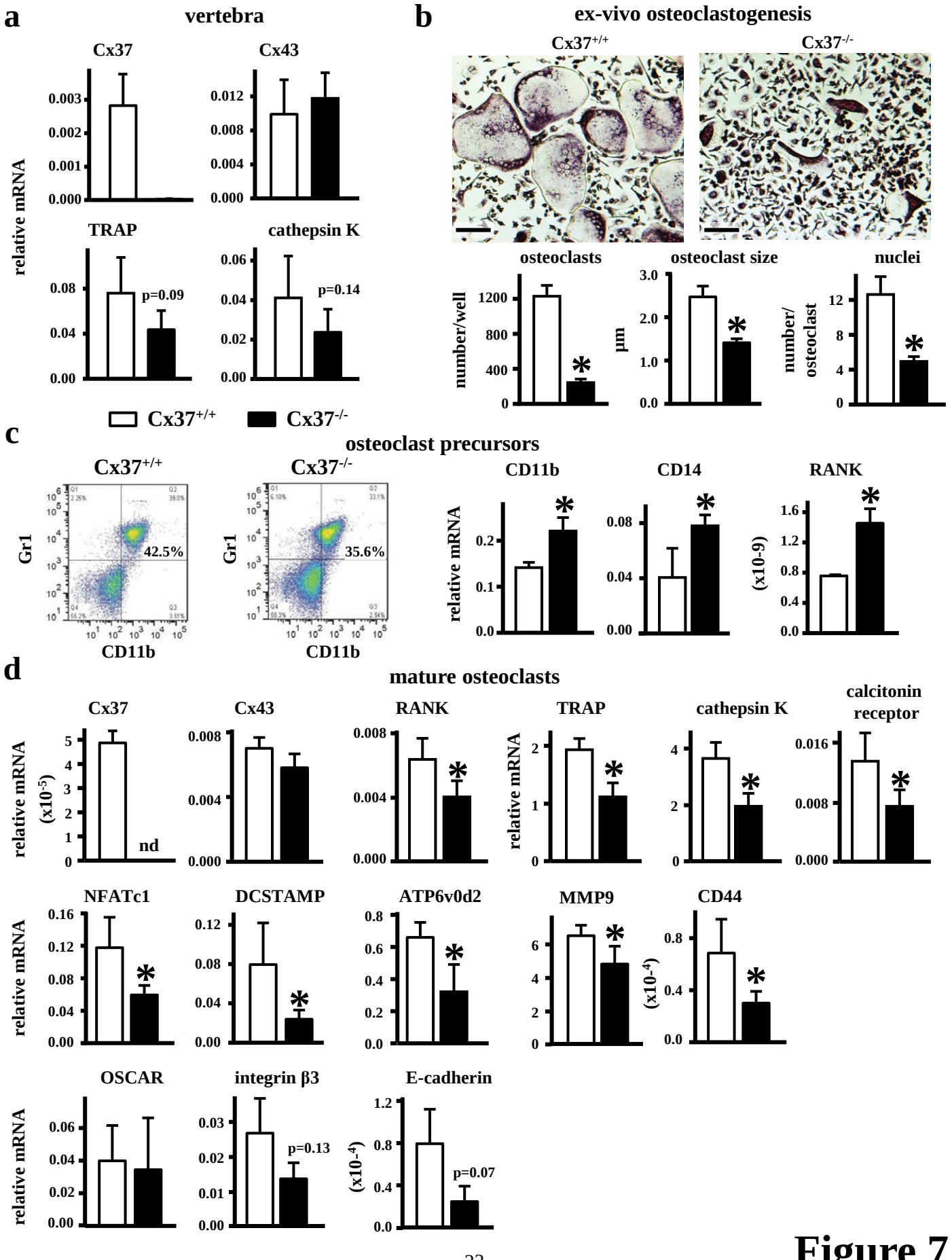
a
vertebra
Cx37
Cx43
TRAP
cathepsin K
relative mRNA
p=0.09
p=0.14
Cx37+/+
Cx37-/-
b
ex-vivo osteoclastogenesis
Cx37+/+
Cx37-/-
osteoclasts
osteoclast size
nuclei
number/well
µm
number/ osteoclast
c
osteoclast precursors
Cx37+/+
Cx37-/-
Gr1
CD11b
42.5%
35.6%
CD11b
CD14
RANK
relative mRNA
(x10-9)
d
mature osteoclasts
Cx37
Cx43
RANK
TRAP
cathepsin K
calcitonin receptor
relative mRNA
(x10-5)
nd
NFATc1
DCSTAMP
ATP6v0d2
MMP9
CD44
(x10-4)
OSCAR
integrin β3
E-cadherin
p=0.13
p=0.07

Figure 7

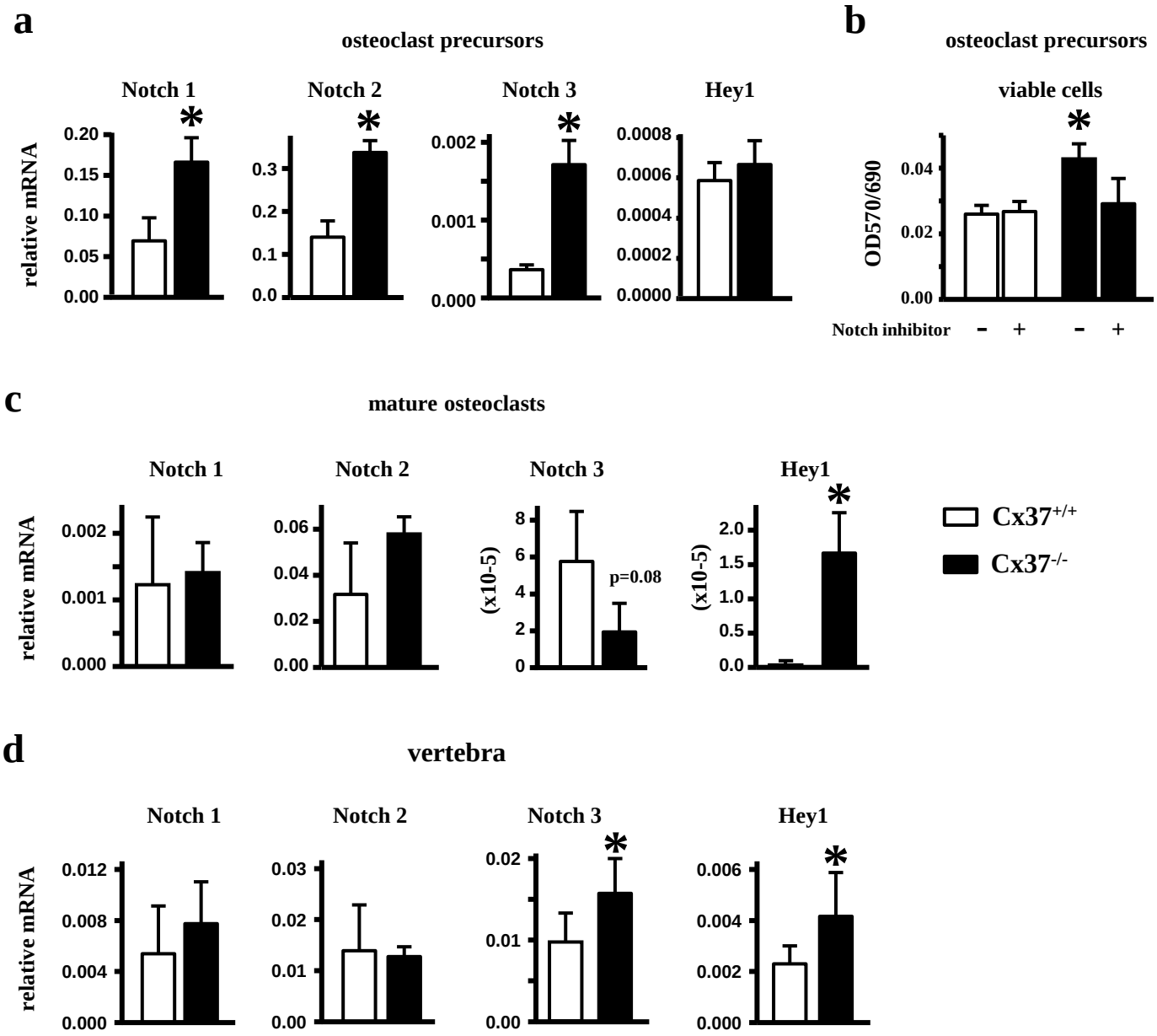
a
osteoclast precursors
Notch 1
Notch 2
Notch 3
Hey1
relative mRNA
b
osteoclast precursors
viable cells
OD570/690
Notch inhibitor
c
mature osteoclasts
Notch 1
Notch 2
Notch 3
Hey1
relative mRNA
(x10-5)
p=0.08
Cx37+/+
Cx37-/-
d
vertebra
Notch 1
Notch 2
Notch 3
Hey1
relative mRNA

Figure 8

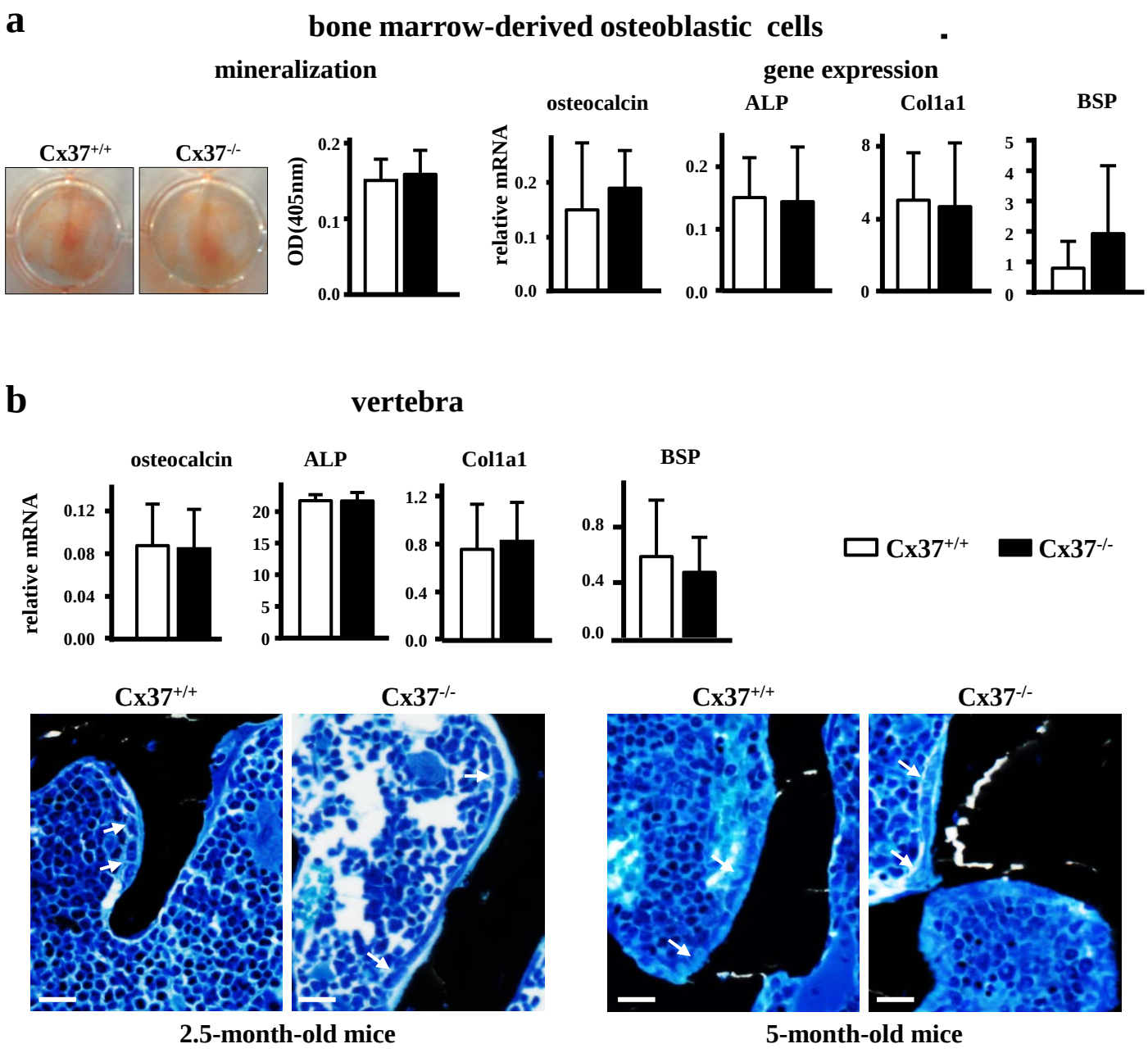
a
bone marrow-derived osteoblastic cells
mineralization
gene expression
Cx37+/+
Cx37-/-
OD(405nm)
relative mRNA
osteocalcin
ALP
Col1a1
BSP
b
vertebra
Cx37+/+
Cx37-/-
2.5-month-old mice
5-month-old mice

Figure 9

Cx37$^{+/+}$

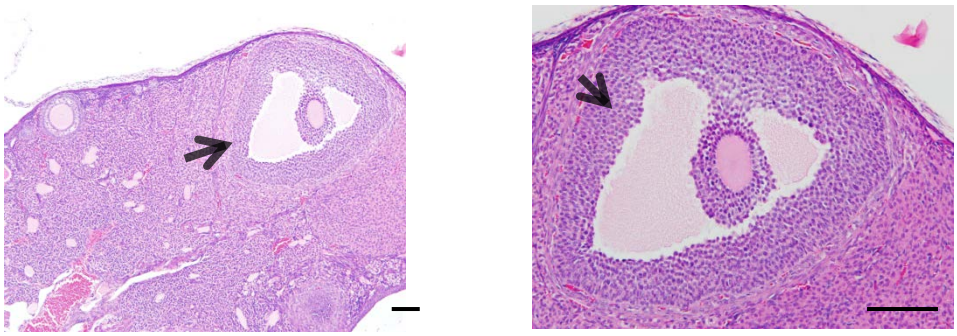

Cx37$^{-/-}$

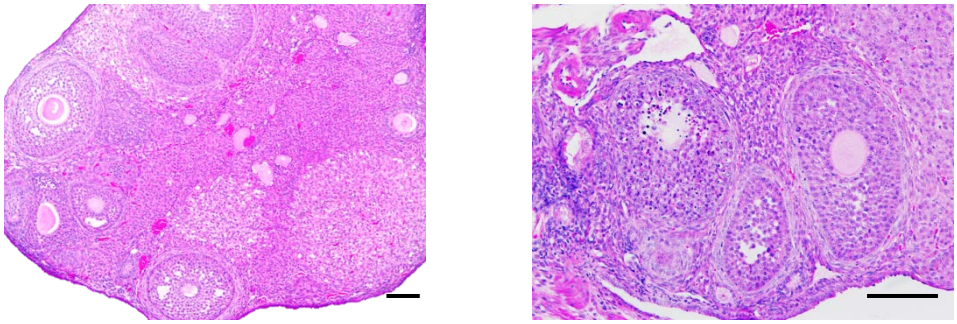

Figure 10